engineering proceedings

MDPI

Proceeding Paper

Extra-Super-Fast Charger for Electric Vehicles (EVs) and Plug-In Hybrid Electric Vehicles (PHEVs) †

Mian Muhammad Amir Ayaz *, Ajmal Farooq * and Ihteshamul Haq *

Department of Electrical Engineering, University of Engineering and Technology, Mardan 23200, Pakistan
* Correspondence: ayazamir94@gmail.com (M.M.A.A.); ajmal@uetmardan.edu.pk (A.F.); ihtesham_afridi20@yahoo.com (I.H.)
† Presented at the 2nd International Conference on Emerging Trends in Electronic and Telecommunication Engineering, Karachi, Pakistan, 15–16 March 2023.

Abstract: The main aim of this study is the development of a fast and secure charging system for electric vehicles. Recently, many different charging methods have been introduced. The main charging methods are the induction charging method and the conduction charging method. In this paper, the conduction charging method is employed. With regard to the conduction method, there are three levels of charging. At level 1, there is single-phase charging, while both single-phase and three-phase charging occur at level 2. Lastly, at level 3, a three-phase AC charging method, DC conduction charging method, and AC/DC conduction charging method is focused. The level 3 charging method is the main focus of this paper. Toward this end, a 12-diode rectifier or 12-pulse rectifier with a firing angle of zero degrees having two bridges is used for AC to DC conversion, while a SEPIC converter is used for DC-to-DC conversion. The design presented in this paper was simulated and verified using MATLAB/Simulink, and the results show that the Total Harmonic Distortion (THD) of the input current was reduced, and that overall efficiency was improved.

Keywords: Total Harmonic Distortion (THD); Single Ended Primary Induction Converter (SEPIC); Electric Vehicles (EVs); Plug-in Hybrid Electric Vehicles (PHEVs)

Citation: Ayaz, M.M.A.; Farooq, A.; Haq, I. Extra-Super-Fast Charger for Electric Vehicles (EVs) and Plug-In Hybrid Electric Vehicles (PHEVs). *Eng. Proc.* **2023**, *32*, 24. https://doi.org/10.3390/engproc2023032024

Academic Editors: Muhammad Faizan Shirazi, Saba Javed, Sundus Ali and Muhammad Imran Aslam

Published: 11 May 2023

1. Introduction

We are living in an era in which air pollution is a significant concern. The cars we use are gasoline-powered vehicles, running on petrol, diesel, or gas. Therefore, these vehicles emit a large amount of air pollution to the environment, consisting of pollutants such as carbon monoxide, nitrogen oxide, benzene, and unburned hydrocarbons with some small amount of matter. When closely examing benzene, one can observe that it contains six carbons and six hydrogens importantly, hybrid bonding between the carbons can easily cause cancer in human beings and animals.

Presently, global warming issues are being exacerbated by gasoline-powered vehicles, so an alternative method should be adopted to overcome the corresponding air pollution. For all these problems, the solution is the adoption of Electric Vehicles (EVs), Plug-in Hybrid Electric Vehicles (PHEVs), and Hybrid Electric Vehicles (HEVs). Recently, universities have applied initiatives for charging systems to improve renewable energy systems [1].

First, HEVs, these vehicles contain internal combustion energy system and a battery for powering the vehicle. HEVs reduce energy losses [2]. While gas-powered vehicles lose energy with each pump of the brakes, HEVs utilize this type of energy by employing regenerative braking. In this system, energy is stored in the battery by the regenerative braking system. Second, concerning PHEVs, these vehicles have both a combustion engine and a battery. In a hybrid car, the battery and the engine are connected, while in the case of a plug-in hybrid system, these two systems operate separately [2]. Third, regarding EVs, these vehicles do not contain a combustion engine. In EVs, the driving range depends

on the vehicle's battery size [2]. So, by comparing EVs' charging systems with respect to the distance covered by combustion engines, it can be found that EVs are economically superior. Specifically, 60% savings in fuel cost can be obtained when using an electric car instead of a combustion engine [3,4]. The maintenance cost of EVs is 40% less than their competitors [5,6].

For the efficient adoption of EVs, a protective device for the charging system should be implemented to improve the battery-charging process. In today's world, the types of charging systems used in EVs are mainly DC-powered, whereas our power grids provide us with AC Power. So that should be converted to DC. In this paper, we provide a brief overview of an experiment wherein the voltage from the grid will be decremented; then, this decrement will be further imposed in a six-phase charging system to obtain a 60-degree phase difference with every adjacent phase and with equal magnitude of each phase. Figure 1 shows how the charging system functions.

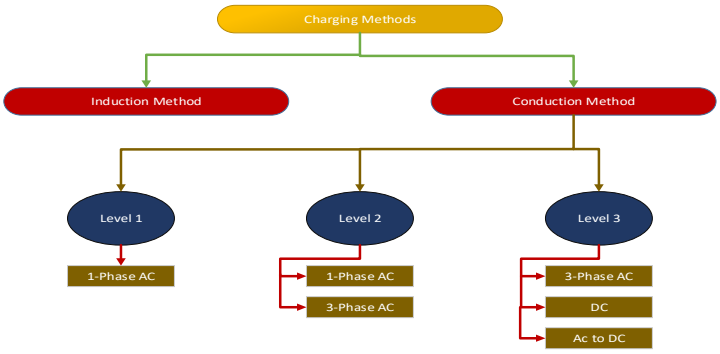

Figure 1. Types of charging methods.

Two types of charging systems are presented in the [5] block diagram of Figure 1.

The primary focus in this study will be on level 3 with improved input THD for current. At this level of an EV-charging scheme, the grid, AC/DC converter, boost converter, and a charging port are connected [1]. A five-level battery-charging system for electric vehicle charging to improve their overall efficiency is presented [7,8]. For improving efficiency, a fuzzy-logic-controlled scheme has also been used [9,10]. However, three parallel SEPIC converters are used for DC-to-DC conversion, which confers an improvement in the input current THD. Many researchers are currently attempting to improve the charging systems of EVs [3–17].

2. Proposed System

The proposed model consists of a 12-diode rectifier connected to a DC-to-DC SEPIC converter and different filters, which then provide an efficient output. Figure 2 is proposed model implemented in MATLAB Simulink. The goal of our model is to improve THD, peak-to-peak ripples of output voltage and current, and overall efficiency.

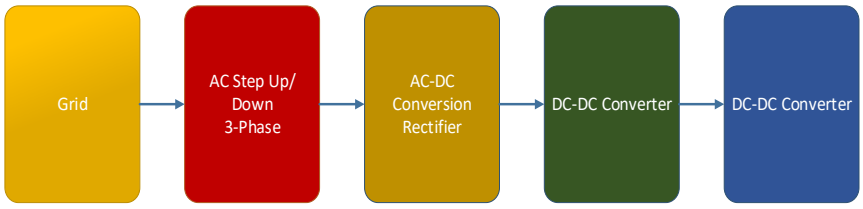

Figure 2. Charging system working steps.

Below Figure 3a, a circuit diagram of the proposed model is shown, which consists of a six-phase winding transformer, a twelve-diode rectifier, and four interleaved SEPIC

converters. For rectification, a special type of transformer that can provide six-phase voltage with a phase difference of 30 degrees is required as shown in Figure 3b.

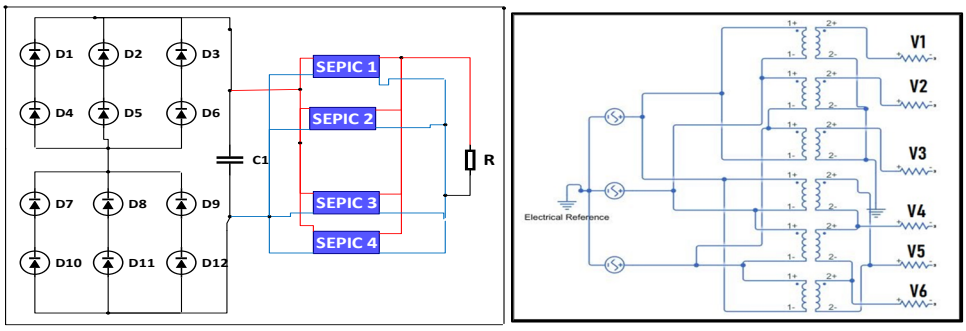

(**a**) (**b**)

Figure 3. Circuitry: (**a**) Proposed Model; (**b**) Three-Winding Transformer.

2.1. Six-Phase, Three-Winding Transformer

A three-winding T/F receives a three-phase input and returns a six-phase output. A diagram of this type of transformer is given in Figure 3b. Since a three-winding T/F has a six-phase output, the phase difference of every phase will be 120 degrees apart, constituting a 60-degree difference between every phase. The input winding is delta and output are star and delta. The O/P of the first three phases will be from star winding, while that of the other three phases will be from delta winding. The three phases of star winding, V1, V2, and V3, will have a 120-degree phase difference between each other. Delta will have same phase difference as star but with a phase shit of 30-degree.

2.2. Pulse Diode Full Uncontrol Rectification

Firstly, in Figure 4a, the mathematical wave for the first diode bridge rectifier is shown, which is Va1.

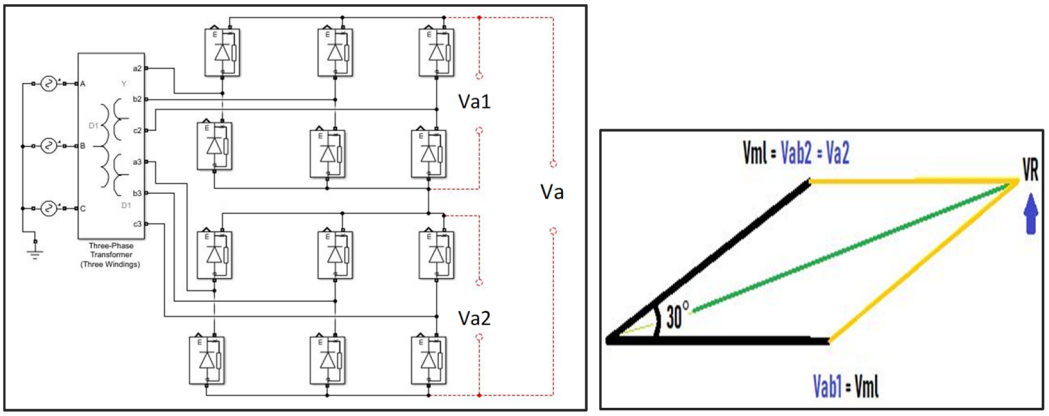

(**a**) (**b**)

Figure 4. Rectification Topology: (**a**) Uncontrolled rectifier; (**b**) Line voltage for star and delta.

The mathematical equation for the diode bridge uncontrolled rectifier Va1 is below:

$$\text{Maxmum line Voltage of Va1} \;=\; \text{Vml (Volt)} \tag{1}$$

$$\text{Minimum line Voltage of Va1} = 0.866\ \text{Vml (Volt)} \tag{2}$$

Both bridges working principles are the same, only difference in 30-degree phase shift between them, which corresponds to Va2 from Figure 4a.

The mathematical formula for second bridge rectifier Va2 is given below:

$$\text{Maxmum line Voltage of Va2} \;=\; \text{Vml (Volt)} \tag{3}$$

$$\text{Minimum line Voltage of Va2} = 0.866\ \text{Vml (Volt)} \tag{4}$$

By adding Equations (2) and (4), result becomes Equation (7). For the calculation of the resultant line voltage, we use the vector calculation property. First, consider Figure 4a.

From Figure 4b, we can obtain the following vector equations.

$$\text{Va1} \;=\; \text{Va2} \;=\; \text{Vml} \tag{5}$$

$$\text{VR} = \text{Vr} = \sqrt{\text{Vml}^2 + \text{Vml}^2 + 2\text{Vml}^2\cos 30^\circ} \tag{6}$$

$$\text{Vr} = \text{Vp} = 1.932\ \text{Vml (Volt)} \tag{7}$$

The resultant Voltage from the mathematical equation is about 1.932 Vml Volts.

The voltage is calculated and compared with the Simulink scope graph value. Therefore, following mathematical calculations are used:

$$\text{Va} = \frac{1}{\left(\frac{\pi}{6}\right)} \int_{90-15}^{90+15} \text{Vp} \sin\ \omega t\, dt \tag{8}$$

$$\text{Va} = 734.16\ \text{(Volt)} \tag{9}$$

The line voltage in our system coming from the 12-pulse uncontrolled diode bridge rectifier is about 380 V. After the calculations, we can see that the resultant voltage is 734.16 V. By comparing this value with Figure 3b, the rectifier voltage has been determined through MATALAB/Simulink Scope, yielding an average voltage of about 730 Volts.

2.3. DC-to-DC Converter

A SEPIC converter is for DC-DC conversion to increase or decrease DC Voltage or deliver same output as input. The output of the SEPIC converter is controlled by duty cycle via a switch. Maximum voltage occurs at 90% of the duty cycle. It has a similar output to a Cuk-Converter, with the only difference being the output polarity. In a SEPIC converter, the efficiency of voltage is superior to that of other converters such as a buck converter, a boost converter, etc.; thus, it is economically than other DC-DC converters.

The mathematical equation for SEPIC obtained from Figure 5 is given below:

$$\text{Vr} = \text{Vs}\left(\frac{\text{D}}{1-\text{D}}\right),\ \text{Vr} = \text{Resistance Voltage} \tag{10}$$

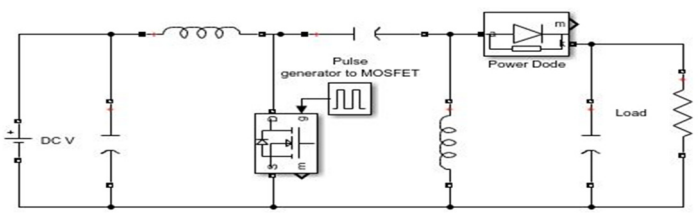

Figure 5. SEPIC DC-to-DC Converter.

2.4. Mathematical Formulae for Proposed Model

The 12-pulse voltage with a firing angle of zero degrees is given below:

$$\mathrm{Va} = \frac{1}{\left(\frac{\pi}{6}\right)} \int_{90-15}^{90+15} \mathrm{Vp} \sin\ \omega t \, dt \tag{11}$$

$$\mathrm{Va} = 734.16\ (\mathrm{Volt}) \tag{12}$$

The SEPIC formula for voltage is given below:

$$\mathrm{Vr} = \mathrm{Vs}\left(\frac{\mathrm{D}}{1-\mathrm{D}}\right) \tag{13}$$

$$\mathrm{Vr} = 734\left(\frac{0.5}{1-0.5}\right) = 734\ \mathrm{Volt} \tag{14}$$

From the output voltage of the calculation, it can be observed that the voltage is 734 Volts, which is exactly related to our proposed model, which also yields a value of about 730 Volts. The current is about 35 A as determined via Simulink.

3. Simulation Results

The output waveform of the three winding T/F is given in Figure 6a. The three-phase line voltage of the star in (T/F) output wave is given in Figure 6b, along with the 30-degree phase shift of the delta waveform. Figure 6b presents the line voltage, which, in a delta connection, is the same as the phase voltage. In Figure 6a,b the numbers of coordinates at y-axis are amplitude of voltage in Volts while as x-axis is time in seconds.

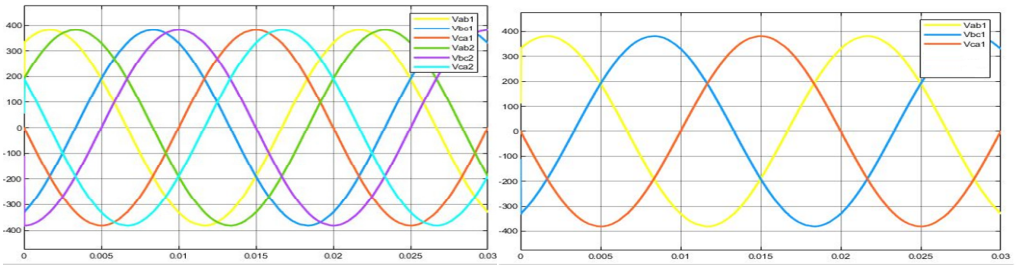

(**a**) (**b**)

Figure 6. (**a**) Voltage of three-winding transformer; (**b**) Star connection voltage.

Figure 6a presents six equal magnitudes of 220 V and a phase difference of 120 degrees. The following graphs have been taken from the MATLAB Simulink model of the three-winding transformer designed for our research. Figure 7a shows a phase shift when compared to Figure 6b; this is because the waveform of Figure 7a is the output of the delta winding of the transformer. Figure 7b presents the maximum line voltage and the minimum line voltage. In Figure 7a,b the number of coordinates at y-axis shows the voltage magnitude in Volts while x-axis coordinate is time in seconds.

Figure 8a presents a line voltage of Va2 with a phase shift of 30 degrees. This phase shift occurs because of the line voltage coming from the delta connection of the transformer. In Figure 8a,b the number of coordinates at y-axis are magnitude of voltage in Volts while x-axis coordinates are time in seconds.

The resultant wave in Figure 8b has a phase difference of 15 degrees. This means that the overall Va corresponds to the rectifier voltage of the pure 12-diode rectifier.

Figure 8a shows a line voltage of Va2 with a phase shift of 30 degrees. Hence, in Figures 7b and 8a, both bridges have the same property as it rectifies the voltage coming from (T/F). Every bridge gives an output with a 60-degree phase difference.

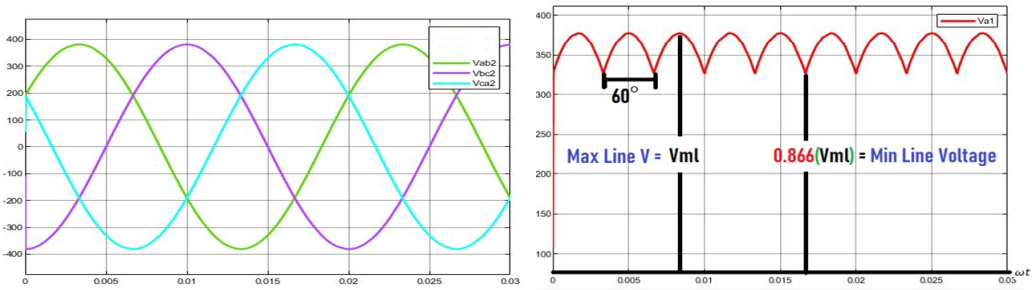

(**a**) (**b**)

Figure 7. T/F O/P Signal: (**a**) Delta connection Voltage; (**b**) Va1 Voltage Wave Form.

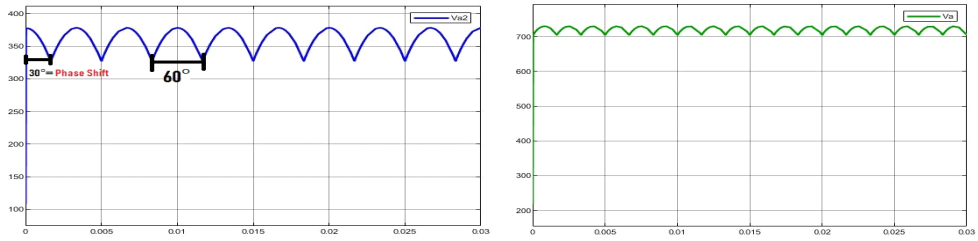

(**a**) (**b**)

Figure 8. (**a**) Rectifier VolategeVa2 voltage wave form; (**b**) Rectifier output voltage.

The rectifier's average voltage is about 730 Volts. By adding a capacitor to the output of the rectifier, we obtain the resultant voltage reading wave given in Figure 9a. The THD of the input current was determined through FFT analysis via MATLAB Simulink as in Figure 9b. In Figure 9b, it is clear that the input current THD is about 1.13%, which is a good improvement. The green line in Figure 9a shows that by adding a capacitor after rectifier in parallel the voltage magnitude becomes smother as compared to Figure 8b. The blue line of Figure 9b shows that the total harmonic distortion of input current is 1.13% with respect to fundamental frequency of 50 Hz. In Figure 9a the y-axis coordinate is magnitude of voltage in Volts and x-axis coordinate is time in seconds.

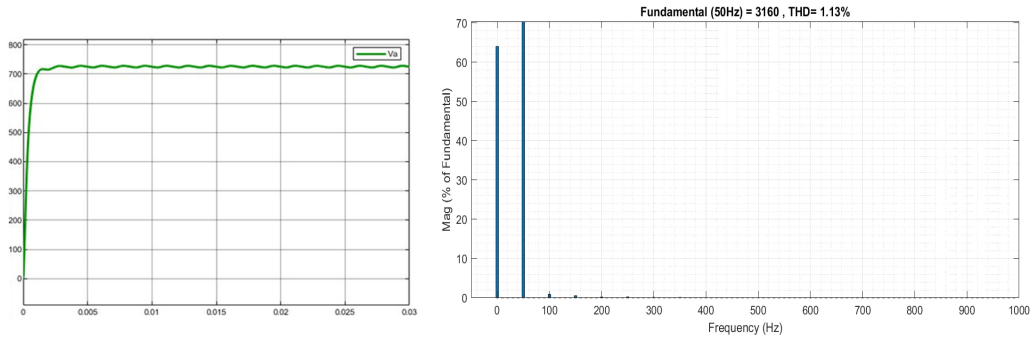

(**a**) (**b**)

Figure 9. (**a**) Rectifier O/P voltage with capacitor; (**b**) Input current THD analysis.

In Figure 10a, the peak-to-peak output voltage was determined from the proposed Simulink model. In Figure 10b, the value of the peak-to-peak ripples of voltages is equal to 0.15 Volts. The average O/P voltage is about 700 Volts, which was adjusted through bar-related DC component. In Figure 10a the red straight line is O/P voltage of proposed system.

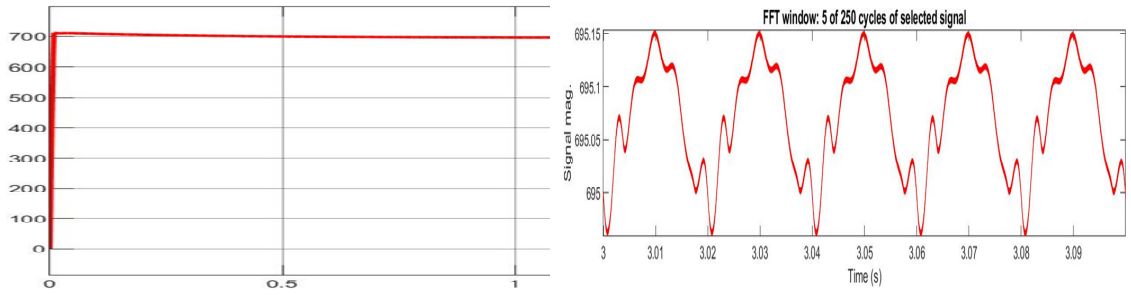

(**a**) (**b**)

Figure 10. O/P Voltage: (**a**) O/P Voltage from Simulink; (**b**) Peak-Peak O/P Voltage.

In Figure 11a, the value of the peak-to-peak ripples of output current is about 0.001 Amps. In Figure 11a,b the y-axis coordinate is magnitude of current in ampere and x-axis coordinate is time in seconds. In Figure 11b the current is pulsating DC current with very less peak-to-peak ripple difference for charging system of EVs and PHEVs. Figure 11a,b both are output current with improved in peak-to-peak ripples in current. In Figure 11b the blue line is O/P current of proposed system.

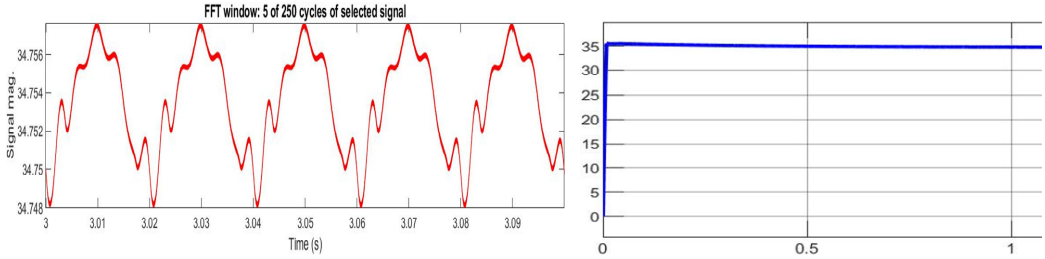

(**a**) (**b**)

Figure 11. O/P Current: (**a**) Peak-Peak O/P Current; (**b**) Output current.

4. Discussion and Comparative Analysis

The following table shows different readings taken from the Simulink models without filters.

In Table 1, there are four different types of modified DC-to-DC converters. The first one is an SEPIC converter with three connections in parallel, which gives the required result (as shown in the table). These readings have been taken from MATLAB/Simulink. The second reading in Table 1 is of a four-series SEPIC converter with connected in a cascaded series, which means that the first output is the input of the second and vice versa.

Table 1. Comparative Analysis without Filter.

Name/Without Filter	Input Current THD	Rectifier O/P Voltage	Rectifier O/P Current
3-Parallel SEPIC with 12 Pulse	43.7%	421.4 V	63 A
4-Series SEPIC with 12 Pulse	43.46%	365 V	358 A
4-Parallel SEPIC with 12 Pulse	43.69%	424 V	62.51 A
4-Parallel SEPIC with 3-Phase Full uncontrolled Rectifier	158.62%	366.7 V	53.99 A

Table 2 shows different readings of the peak-to-peak ripple current of the rectifier output, the peak-to-peak ripple voltage of the rectifier output, the output voltage, and the input voltages extracted from different Simulink models.

Table 2. Comparative Analysis with Different Topologies Output Voltage and Current.

Name	Rectifier O/P Voltage Peak-to-Peak Ripples	Rectifier O/P Current Peak-to-Peak Ripples	O/P Voltage	O/P Current
3-Parallel SEPIC with 12 Pulse	430 − 400 = 30 Vp-p	100 Ap-p	643.7 V	32.14 A
4-Series SEPIC with 12 Pulse	450 − 250 = 200 Vp-p	1500 Ap-p	1349 V	67.42 A
4-Parallel SEPIC with 12 Pulse	450 − 500 = 50 Vp-p	200 Ap-p	695.1 V	34.75 A
4-Parallel SEPIC with 3-Phase Full uncontrolled Rectifier	375 − 355 = 20 Vp-p	300 Ap-p	600 V	30 A

Table 3 shows the readings of the proposed system, which were implemented in and taken from MATLAB/Simulink.

Table 3. Comparative Analysis with Different Topologies.

Name	O/P Voltage Peak-Peak Ripples	O/P Current Peak-Peak Ripples	O/P V & I THD Bar Related DC
3-Parallel SEPIC with 12 Pulse	644.5 − 643 = 1.5 V	32.22 − 32.16 = 0.006 A	0.11%
4-Series SEPIC with 12 Pulse	1352 − 1346 = 6 V	67.6 − 67.3 = 0.3 A	0.29%
4-Parallel SEPIC with 12 Pulse	695.1 − 695 = 0.1 V	34.756 − 34.74 = 0.008A	0.01%
4-Parallel SEPIC with 3-Phase Full uncontrolled Rectifier	600.3 − 600.26 = 0.04 V	30.015 − 30.013 = 0.002 A	0%

Table 4 proposed system with improved THD and O/P voltage peak-peak ripples. Table 4 below indicates that providing an O/P voltage 220 V rms to the charger will give about 700 V to the battery or load. Thus, the THD is improved.

Table 4. Proposed System Total Harmonic Distortion and Peak to Peak Ripples at Output.

THD of Input Current	1.13%
Input Voltage	220 V rms
Output Voltage Peak-to-Peak Ripples	695.15 − 695 = 0.15 V
Output Current Peak-to-Peak Ripples	34.756 − 34.748 = 0.008 A
Output Voltage to Load	Approximately 695 V = 700 V

5. Conclusions

In this paper, an extra-super-fast charging system has been modeled for EVs and PHEVs through MATLAB/Simulink. The comparative analysis and results show that the THD of the input current is greatly reduced (1.13%), while the output values for the peak-to-peak ripples for voltage and current are greatly reduced and valid for further procedures. In conclusion, the proposed model presented in this paper is a very efficient charging system and can be used when tested practically.

Author Contributions: Conceptualization, M.M.A.A. and A.F.; methodology, M.M.A.A. and A.F.; software, M.M.A.A. and A.F.; validation, M.M.A.A. and A.F.; formal analysis, M.M.A.A. and A.F.; investigation, M.M.A.A. and A.F.; resources, M.M.A.A. and A.F.; data curation M.M.A.A. and A.F.; writing—original draft preparation, M.M.A.A.; writing—review and editing, M.M.A.A. and A.F.; visualization, M.M.A.A. and A.F.; supervision, A.F.; project administration, A.F.; funding acquisition, A.F. and I.H. All authors have read and agreed to the published version of the manuscript.

Funding: This research received no external funding.

Institutional Review Board Statement: Not applicable.

Informed Consent Statement: Not applicable.

Data Availability Statement: The data are discussed in the results of this paper. The overall dataset was simulated and verified through MATLAB/Simulink software.

Conflicts of Interest: The authors declare no conflict of interest.

References

1. Genikomsakis, K.N.; Gutierrez, I.A.; Thomas, D.; Ioakimidis, C.S. Simulation and Design of Fast Charging Infractructure for a university based e-Carsharing system. *IEEE Trans. Intell. Transp. Syst.* **2017**, *19*, 1524–9050.
2. Environment America Clean Air, Clean Water, and Open Source. Available online: https://environmentamerica.org/blogs/environment-america-blog/amc/what-difference-between-hybrid-cars-plug-hybrid-cars-and-electric (accessed on 21 January 2022).
3. Farjah, A.; Bagheri, E.; Seifi, A.R.; Ghanbari, T. Main & Auxiliary Parts of Battery Storage, Aimed to fast charging of EV's. In Proceedings of the 2018 9th annual power electronics drive system and technologies conference (PEDSTC), Tehran, Iran, 13–15 February 2018.
4. Energy Efficiency and Renewable Energy. Available online: https://www.energy.gov/eere/vehicles/articles/fotw-1186-may-17-2021-national-average-cost-fuel-electric-vehicle-about-60 (accessed on 17 May 2021).
5. Alsalemi, A.; Al-Zubiri, A.; Sadeghi, Y.; Massoud, A. The research is on Design of ultra-fast EVs battery charger. In Proceedings of the Symposium on Computer Applications and Industrial Electronics (ISCAIE), Penang, Malaysia, 3–4 April 2021.
6. Yeale School of Environmnet. Available online: https://e360.yale.edu/digest/energy-department-report-finds-that-evs-cost-40-percent-less-to-maintain-than-conventional-cars (accessed on 23 June 2021).
7. Nair, A.C.; Fernandes, B.G. A Solid State Transformer Base Fast Charging Station for all Category of Electric Vehicles. In Proceedings of the IECON 2018-44th Annual Conference of the IEEE Industrial Electronics Society, Washington, DC, USA, 21–23 October 2018.
8. Vinoth, K.K.; Saravanakumar, R. Implementation of Five Level Battery Charging Scheme for Electric Vehicles. In Proceedings of the 2020 International Conference on Power, Instrumentation, Control and Computing (PICC), Thrissur, India, 17–19 December 2020. [CrossRef]
9. Sharma, A.; Gupta, R. Bharat DC001 charging standard based electric vehicles EVs fast charger. In Proceedings of the IECON 2020 The 46th Annual Conference of the IEEE Industrial Electronics Society, Singapore, 18–21 October 2020.
10. Chelladurai, B.; Sundarabalan, C.K.; Santhanam, S.N.; Guerrero, J.M. Interval Type-2 Fuzzy Logic Controlled Shunt Converter Coupled Novel High-Quality Charging Scheme for Electric Vehicles EVs. *IEEE Trans. Ind. Inform.* **2020**, *17*, 6084–6093. [CrossRef]
11. Zan, X.; Xu, G.; Zhao, T.; Wang, R.; Dai, L. Multi Batteries Block Module Power Converter for EV's Driven by Switched Reluctance Motors. *IEEE Access* **2021**, *9*, 140609–140618. [CrossRef]
12. Guerriero, P.; Coppola, M.; Lauria, D.; Daliento, S. PWM Based Sliding Mode Control of a fast-charging charger for supercapacitors. In Proceedings of the 2020 International Symposium on Power Electronics, Electrical Drives, Automation and Motion (ISPEEDAM), Sorrento, Italy, 24–26 June 2020.
13. Ahn, J.H.; Lee, B.K. High Efficiency Adaptive-Current Charging Strategy for Electric Vehicles EVs Considering Variations of Internal Resistance of Lithium-ion Battery. *IEEE Trans. Power Electron.* **2018**, *34*, 3041–3052. [CrossRef]
14. Gaurav, A.; Gaur, A. The research title is on Modelling of Hybrid Electric Vehicle EVs Charger and Study the Simulation Results. In Proceedings of the 2020 International Conference on Emerging Frontiers in Electrical and Electronic Technologies (ICEFEET), Patna, India, 10–11 July 2020.
15. Kravetz, F.I.; Gules, R. Soft-Switching High Static Gain Modified SEPIC Converter. Citation information. *IEEE J. Emerg. Sel. Top. Power Electron.* **2021**, *9*, 6739–6747. [CrossRef]
16. Farooq, A.; He, C.; Chen, G. A Three Phase Interleaved Boost Converter with L & C Extension Mechanism. *Tech. Gaz.* **2018**, *25*, 52–59.
17. Farooq, A.; Malik, Z.; Sun, Z.; Chen, G. A Review of Non-isolated High Step-down dc-dc Converters. *Int. J. Smart Home* **2015**, *9*, 133–150. [CrossRef]